Desalination and Water Treatment
www.deswater.com
doi: 10.1080/19443994.2015.1094423

57 (2016) 18897–18905
August

Taylor & Francis
Taylor & Francis Group

Photocatalytic treatment of colored wastewater from medical laboratories: photodegradation of Nuclear Fast Red

E. Deletze[a], A. Antoniadis[a], V. Kitsiou[a], E. Kostopoulou[b], D. Lutic[c], I. Cretescu[d], I. Poulios[a,*]

[a]*Laboratory of Physical Chemistry, Department of Chemistry, Aristotle University of Thessaloniki, 54124 Thessaloniki, Greece, Tel. +30 2310 997785; Fax: +30 2310 997709; email: edeletze@chem.auth.gr (E. Deletze), aanton@chem.auth.gr (A. Antoniadis), vasso_k3@hotmail.com (V. Kitsiou), poulios@chem.auth.gr (I. Poulios)*
[b]*Pathology Department, University of Thessaly, 41110 Larisa, Greece, email: ekosto@med.uth.gr*
[c]*Faculty of Chemistry, Alexandru Ioan Cuza University, 11 Carol I Boulevard, 700506 Iasi, Romania, email: doilub@yahoo.com*
[d]*Faculty of Chemical Engineering and Environmental Protection, Department of Environmental Engineering and Management, Gheorghe Asachi Technical University of Iasi, 73 Professor D. Mangeron Street, 700050 Iasi, Romania, email: icre1@yahoo.co.uk*

Received 5 March 2015; Accepted 5 September 2015

ABSTRACT

The degradation and organic content reduction of Nuclear Fast Red (NFR, a counterstain reagent widely used in biochemical and biomedical laboratories) in aqueous solutions has been studied by heterogeneous photocatalytic oxidation under artificial irradiation. For the heterogeneous processes, the performance of different commercial titanium oxides on the degradation and the organic content reduction (DOC) of the wastewater was examined. The decomposition of the NFR follows quite well a pseudo-first kinetic order in the whole pH range, in line with the Langmuir–Hinshelwood model. The effects of catalyst concentration, of the initial solution pH and of H_2O_2 concentration upon the reaction rate, were also investigated. NFR degradation was accompanied by the formation of ammonium, nitrate, and sulfate ions, as they have been detected as mineralization products in the liquid phase.

Keywords: Photocatalysis; Nuclear fast red; Photodegradation; Dyes; TiO_2

1. Introduction

The elimination of toxic chemicals from wastewater is nowadays a very important subject in pollution control. The pollutants originate in various industries (petroleum refining, textile processing, etc.), agriculture (pesticides, fertilizers), as well as household and personal care areas (tensioactives, detergents, pigments, dyes, odorizers, etc.); several of these are resistant to conventional chemical and biological wastewater treatment technologies [1–3]. The need for alternative methods is of interest to regulating authorities everywhere. The increased concern for the use of the advanced oxidation processes (AOPs), such as heterogeneous photocatalysis (TiO_2/UV-A), ozonation, H_2O_2/UV-B, photo-Fenton, etc., may be explained by the need for seeking of new, alternative to the conventional ones, and environmentally friendly technologies [4,5].

Concerning heterogeneous photocatalysis, it has been demonstrated that the use of semiconducting materials mediating the photocatalytic oxidation of

---

*Corresponding author.

organic compounds can be an alternative to conventional methods for the removal of organic pollutants from water and wastewater. General description of heterogeneous photocatalysis in the presence of TiO_2 under artificial or solar irradiation is presented in several excellent review articles [6,7]. In brief, by the irradiation of an aqueous TiO_2 suspension with light energy greater than the band gap energy of the semiconductor ($E_g > 3.2$ eV), conduction band electrons (e^-) and valence band holes (h^+) are generated. Part of the photogenerated carriers recombine in the bulk of the semiconductor, while the rest reach the surface, where the holes, as well as the electrons, act as powerful oxidants and reductants, respectively. The photogenerated electrons react with the adsorbed molecular O_2 on the Ti(III)-sites, reducing it to superoxide radical anion $O_2^{\cdot -}$, while the photogenerated holes can oxidize either the organic molecules directly or the OH^- ions and the H_2O molecules adsorbed at the TiO_2 surface to $OH^{\cdot}$ radicals. These radicals together with other highly oxidant species (e.g., peroxide radicals) are reported to be responsible for the primary oxidizing step in photocatalysis. The $OH^{\cdot}$ radicals formed on the illuminated semiconductor surface, with a standard reduction potential of 2.8 V, can easily attack the adsorbed organic molecules or those located close to the surface of the catalyst, leading finally to their complete mineralization. A significant advantage of the photocatalytic process is its environmentally friendly character, since it can be mainly powered by the sunlight, reducing significantly the electric power consumption and the operating costs [8,9].

Among various semiconducting materials (oxides, sulfides, etc.), most attention has been paid to TiO_2 (anatase) because of its high photocatalytic activity, resistance to photocorrosion, and relatively low cost.

This study presents results concerning the photocatalytic degradation and mineralization of Nuclear Fast Red (NFR) (Fig. 1), an anthraquinone-derivative dye, over TiO_2 photocatalysts under various experimental conditions.

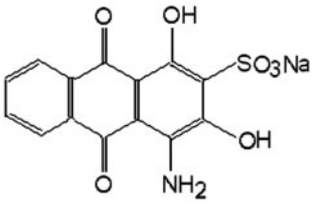

Fig. 1. NFR chemical structure (CAS Number: 6409-77-4).

NFR is a widely used red nuclear counterstain dye in the routine staining of histological tissue sections (several types of cells, etc.). Together with auramine O, hematoxylin, rose bengal, etc., NFR is widely used in biomedical research laboratories and also for diagnostic purposes. Some of these stains are known to be toxic or mutagenic for human and animals [10,11].

According to our knowledge, the methodology mainly used for the removal of these biological stains from solutions is their sorption, either on activated carbon or on a polymeric resin (i.e. Amberlite XAD-16). However, the problem is not solved; the dye is only immobilized on the solid phase [11]. For these reasons, the main objective of this new study was to investigate the possibilities for the elimination of NFR from wastewaters, by photocatalytic oxidation, before their release to the environment. According to the literature, various research groups dealt with the degradation and mineralization of dyes in the presence of UV-A or visible light radiation [12–18] with very promising results.

2. Experimental

2.1. Reagents

NFR ($C_{14}H_8NO_7SNa$, MW 357.28) was provided by Sigma Chemie GmbH and used as received. Various commercial TiO_2 (CAS 6409-77-4) catalysts were used for the photocatalytic experiments such as TiO_2 P-25 Degussa (70/30 anatase/rutile, 55 $m^2 g^{-1}$ BET), TiO_2 Kronos 7000 (TiO_2 K-7000, 100% anatase, >250 $m^2 g^{-1}$ BET), and TiO_2 Millenium (TiO_2-M, 100% anatase, 10 $m^2 g^{-1}$ BET). NaOH (CAS 1310-73-2) and H_2SO_4 (7664-93-9) from Sigma-Aldrich were used for the pH adjustment.

2.2. Procedures and analysis

The experiments were performed in a closed Pyrex cell of 0.5 L capacity. The reaction vessel was fitted with a central 9 W lamp and had inlet and outlet ports for gas bubbling during the reaction. The spectral response of the irradiation source (OsramDulux S 9 W/78, UVA), according to the supplier, ranges between 350 and 400 nm, with a maximum at 366 nm and two additional weak lines in the visible region. The photon flow per unit volume of the incident light was determined by chemical actinometry using potassium ferrioxalate (CAS 15375-82-3) [19]. The initial light flux, under exactly the same conditions as in the photocatalytic experiments, was evaluated to be 0.93×10^{-4} Einstein $L^{-1} min^{-1}$.

The typical procedure comprised mixing 450 mL of NFR solution with the appropriate amount of semiconductor powder, under magnetic stirring, before and during the irradiation, while purging the solution with CO_2-free air. Prior to the photocatalytic experiment, the suspension was stirred for 30 min in the dark, in order to achieve the maximum adsorption of the dye onto the semiconductor surface. At specific time intervals, samples from reaction suspension of 5 mL were withdrawn with a syringe. In order to remove the TiO_2 particles, the solution was filtered through a 0.45-μm filter (Schleicher and Schuell). The concentration changes of the NFR were measured from its characteristic absorption band, using a UV–visible spectrophotometer (Shimadzu UV-1700). The pH value of the solution influences in a significant degree, the maximum wavelength for the radiation absorption. Therefore, the photodecomposition of NFR was monitored at pH values of 4.8 and 3 at 518 nm and, respectively, at 536 nm for the pH values of 7.5 and 10.

The extent of mineralization on samples taken at certain time intervals was measured using a TOC Analyser (Shimadzu Instruments, model VCSH TOC Analyser).

SO_4^{2-}, NO_3^-, NO_2^-, and NH_4^+ ions, produced during the photocatalytic oxidation, were determined in a Shimadzu system consisting of an LC-10 AD pump, a CDD-6A conductometric detector (0.25 μL flow-cell), and a CTO-10A column oven. Cations were separated on an Alltech Universal cation column (100 mm × 4.6 mm) preceded by a guard column (7.5 mm × 4.6 mm) of the same material using 3 mM methane sulfonic acid at 1.5 mL min^{-1} constant flow. Anions were separated on an Alltech Allsep anion column (100 mm × 4.6 mm) preceded by a guard column (7.5 mm × 4.6 mm) of the same material using a phthalic acid and lithium hydroxide mixture of 4 mM (pH 4.00) at 1.5 mL min^{-1} constant flow. Column and conductivity cell temperatures were held constant at 35 and 38˚C, respectively. Calibration curves (0.01–10 mg L^{-1}) were constructed for each ion. The method detection limits were 0.03 mg L^{-1} for NH_4^+ and 0.03, 0.07 mg L^{-1} for NO_3^-, SO_4^{2-}, respectively.

Most of the photocatalytic experiments were carried out at the initial pH value of 4.8, and the reaction temperature was kept constant at 25 ± 0.1˚C.

Some photocatalytic experiments were repeated three times for the sake of reproducibility checking of the experimental results. The accuracy of the optical density values was within ±5%, while the diluted organic carbon reduction during the mineralization experiments was ±10%.

3. Results and discussion

3.1. Photodecomposition of NFR

A first series of experiments of the photocatalytic decomposition of NFR was performed on solutions containing an initial concentration of 30 mg L^{-1} of the dye, in the presence of various commercial TiO_2 catalysts. The concentration of the organic molecule in the solution is plotted against the irradiation time and the results are displayed in Fig. 2.

The exposure of an air-equilibrated NFR solution in the presence of light and the semiconducting powders resulted in a quite fast disappearance of the colored part of the dye molecule. The strong decrease of the characteristic absorption peak indicated that the chromophore, included in the conjugated system with the amino group and the three aromatic rings, was broken.

Under the fore-mentioned experimental conditions, the decolorization of the solution occurred very fast. TiO_2 P-25 and TiO_2 K-7000 showed the same catalytic activity and after 45 min of irradiation, the degradation of the dye in the solution was complete. TiO_2-M, on the other hand, in the same irradiation time leads to an 80% degradation of the molecule. Data from Fig. 2 show that for all C-t curves, the process occurs in two distinctive steps, a fast one in the beginning, followed by a slower phase when reaching a concentration of 60–70% from the initial value.

The stability of the dye to the light was investigated by measuring the dye concentration under irradiation, in the absence of any catalyst. After 2 h of reaction, the direct photolysis yield was less than 10%,

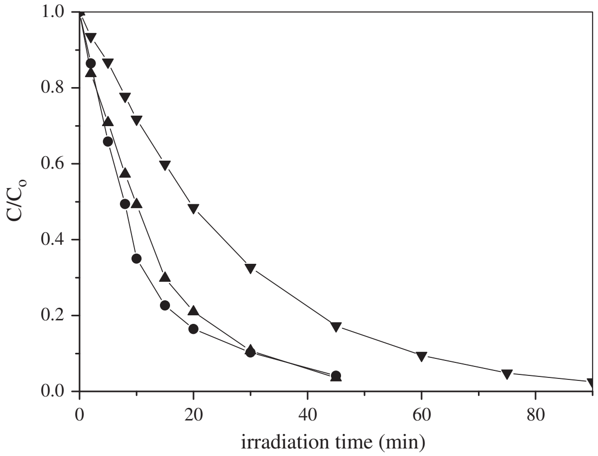

Fig. 2. Photocatalytic degradation of 30 mg L^{-1} NFR at pH 4.8 in the presence of 0.1 g L^{-1} (●) TiO_2 P-25, (▲) TiO_2 K-7000, and (▼) TiO_2 M.

so the contribution of the radiation alone in the degradation of NFR in the time scale under study could be considered negligible.

The photocatalyst dose is a very important factor, strongly influencing the degradation of the organic compound. The optimum amount is in close dependence to the nature of the molecule and the photoreactor design [20].

In the next series of experiments, the effect of TiO_2 P-25 concentration on the initial reaction rate (r_o) of degradation of a 30 mg L^{-1} NFR solution has been observed; the results are presented in Fig. 3. The values of the initial photocatalytic reaction rate in relation to the catalyst concentration follow a Langmuir type isotherm, suggesting that r_o might reach a saturation value at higher TiO_2 concentrations, as reported in similar cases [20,21]. In this study, as the data from Fig. 3 indicate, the optimum value for TiO_2 is 0.5 g L^{-1}, while further increase in the amount of TiO_2 leads to a decrease in the efficiency of photodegradation of NFR.

The optimum photocatalyst dose depends on the geometry and the working conditions of the reactor and corresponds to the optimum degree of light absorption. Above this concentration, the suspended particles of the catalysts block the UV-light passage and increase the light scattering. Furthermore, the decrease of the reaction rates at high catalyst concentration is due to other phenomena that may occur, like agglomeration due to particle–particle interactions, involving a loss of surface area available for light-harvesting [22].

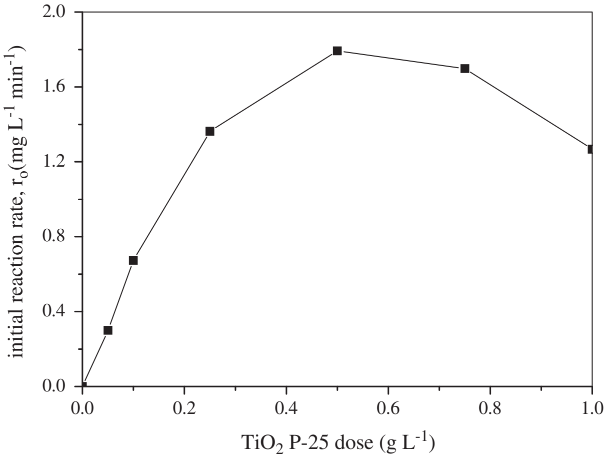

Fig. 3. Influence of the catalyst dose on the initial reaction rate during the photocatalytic degradation of 30 mg L^{-1} NFR at pH 4.8.

3.2. Influence of the NFR concentration and the pH value on the reaction kinetics

The influence of the initial concentration of the solute on the photocatalytic degradation rate of most organic compounds follows a pseudo-first kinetic order, rationalized in terms of the Langmuir–Hinshelwood model (Eq. (1)), modified to describe reactions occurring at a solid–liquid interface [23]:

$$r_o = -\frac{dC}{dt} = \frac{k_r K C_{eq}}{1 + K C_{eq}} \quad (1)$$

where r_o is the initial rate of disappearance of the organic substrate, C_{eq} is the equilibrium bulk-solute concentration, K is the adsorption equilibrium constant for the organic substrate on the solid, and k_r is the limiting reaction rate constant at maximum coverage under the given experimental conditions. This equation can be reorganized to a linear form, easier to operate, as follows:

$$\frac{C_{eq}}{r_o} = \frac{1}{k_r K} + \frac{C_{eq}}{k_r} \quad (2)$$

The pH value appears to play an important role in the photocatalytic process of various pollutants [24–27]. Some properties of the photocatalysts, such as surface charge state and flat band potential, are highly pH dependent, while electrostatic attraction or repulsion between the catalyst's surface and the organic molecule, depending on the ionic form of the organic compound (anionic or cationic), enhances or inhibits, respectively, the photodegradation rate.

The initial reaction rate (r_o) of photodegradation as a function of the equilibrium concentration values of NFR, under different pH values (3, 4.8, 7.5, and 10) is shown in Fig. 4. In the subsequent kinetic study, the equilibrium concentration of the dye (C_{eq}), after 30 min equilibration in the dark was used instead of the initial one (C_o), due to the fact that NFR is adsorbed quite strongly on the TiO_2P-25 surface. The r_o (= $\Delta C/\Delta t$) values were independently obtained by measuring the $C_{eq} - t$ data in the range of 5–50 mg L^{-1} initial NFR concentration during the first 10 min of irradiation, in order to minimize the variations due to the eventual competitive adsorption effects of the intermediates and pH changes associated with the eventual release of H^+ during the photocatalytic reaction. The curves are similar to Langmuir type isotherms; the decomposition rate value increases sharply at low dye concentration and then reaches a plateau associated with saturation at higher concentrations of NFR.

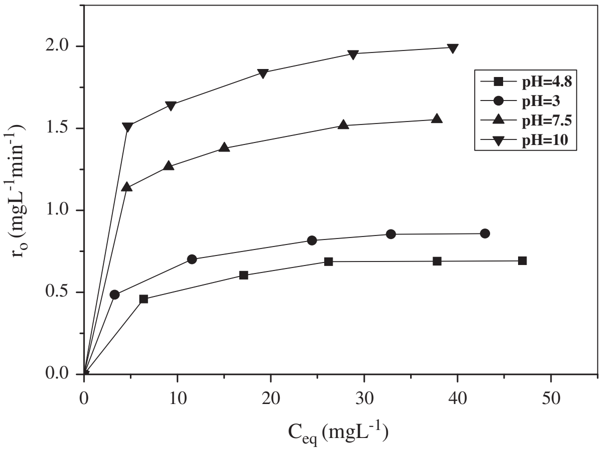

Fig. 4. Initial reaction rate, r_o, of photodegradation vs. initial NFR concentration at different pH values in the presence of 0.1 g L^{-1} TiO_2 P-25.

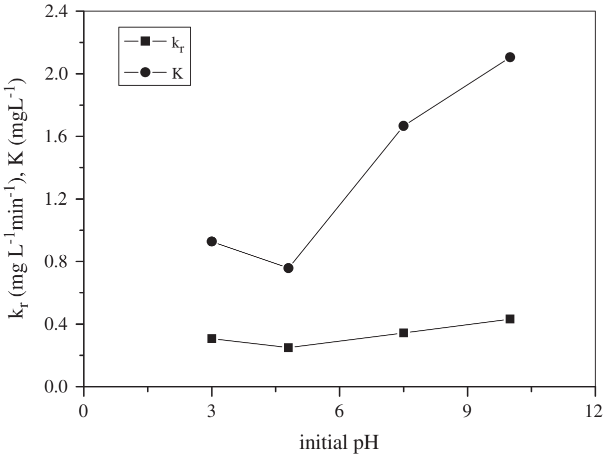

Fig. 6. k_r and K constants for the photocatalytic degradation of 30 mg L^{-1} NFR at different pH values (0.1 g L^{-1} TiO_2 P-25). Data from Fig. 5.

The dependence of C_{eq}/r_o values, according to Eq. (2), on the respective equilibrium concentrations of NFR determined at a constant 0.1 g L^{-1} concentration of TiO_2 P-25 is shown in Fig. 5, while the k_r and K values calculated using the Eq. (2), from the slope of the straight line and from the intercept with the C_{eq}/r_o axis for the different pH values, respectively, are shown in Fig. 6.

The linearity of the curves in Fig. 5 is significant and their slope is consistently different. The dye decolorization rate is higher in the case of basic and neutral, in comparison with the respective ones at lower pH values. It is important to note that even at higher dye concentrations, the linearity is still very good, indicating that the coverage degree of the solid with dye molecules remains reasonable, leaving unaffected the capacity of the solid to interact with UV radiation and initiate the degradation.

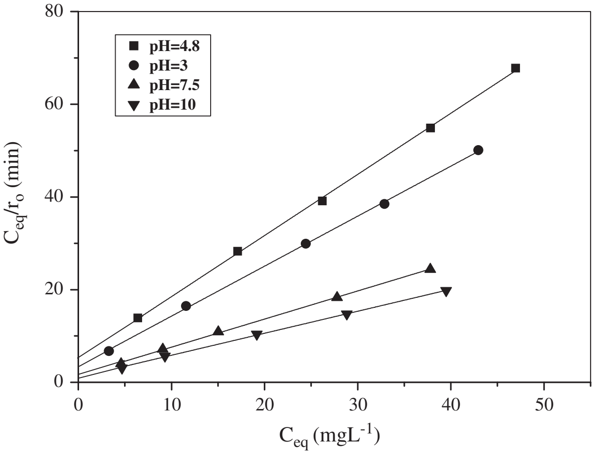

Fig. 5. C_{eq}/r_o vs. C_{eq}, for different pH values in the presence of 0.1 g L^{-1} TiO_2 P-25. Data from Fig. 4.

The effect of pH on the photocatalytic degradation of NFR can be mainly explained by the surface charge of TiO_2 (point of zero charge pzc ≈ 5.6) and its relation to the dissociation constant of $-NH_2$ and of the sulfonic group of NFR, that is a slightly acidic anionic dye.

The less favorable pH value for the photodegradation was proved to be the natural one of 4.8. It is further confirmed by the adsorption equilibrium constant K values in Fig. 6; the lowest value was obtained at pH 4.8. This pH value supposes the slightest adsorption and is associated with the less ionized dye. At both lower and higher pH values, the ionization of $-NH_2$ and $-SO_3Na$ is important. At low pH values, the $-NH_2$ group transforms into $R-NH_3^+$ and the $-SO_3Na$ changes into SO_3H, so the dye becomes itself a Brönsted acid. The non-ionized form is also unfavorable for the reactivity of the dye, since the k_r value reaches a minimum at the 4.8 native pH value of the dye solution. Above this value, both the adsorption constant and the reaction rate increase consistently until pH reaches the value of 10, as shown in Fig. 6.

3.3. Effect of H_2O_2 on the photocatalytic degradation of NFR

The addition of oxidizing species, such as hydrogen peroxide (H_2O_2), potassium peroxydisulfate ($K_2S_2O_8$), and others to TiO_2 suspensions, is a well-known procedure to increase the rate of photooxidation [28,29].

In our case, the photocatalytic degradation of 30 mg L^{-1} NFR in the presence of 0.1 g L^{-1} TiO_2 P-25 at pH of 4.8 has been studied at different H_2O_2 concentrations (Fig. 7). The reaction kinetics were similar to those observed without the oxidants.

The role of H_2O_2 in the photocatalytic degradation is dual: it accepts a photogenerated electron from the conduction band and thus promotes the charge separation (Eq. (3)), or interacts with the O_2^- species, forming $OH^{\bullet}$ radicals via the superoxide mechanism (Eq. (4)):

$$H_2O_2 + e^- \rightarrow HO^- + HO^{\bullet} \quad (3)$$

$$H_2O_2 + O_2^- \rightarrow HO^{\bullet} + HO^- + O_2 \quad (4)$$

The photogenerated intermediates are very active and a reaction with another H_2O_2 molecule cannot be excluded. If an excess of H_2O_2 exists in the reaction medium, it may act as a hole, or $HO^{\bullet}$ scavenger or it can react with TiO_2 to form peroxo-compounds. These are detrimental to the photocatalytic action, competing with the organic compound for the adsorption sites on the catalyst surface. An optimal concentration of H_2O_2 for the maximum effect should be therefore determined [30].

The effect of H_2O_2 concentration on the initial r_o shows that the use of H_2O_2 as an electron scavenger in concentrations from 25 to 150 mg L^{-1} (0.69–4.16 mmol L^{-1}), corresponding to molar ratios H_2O_2: NFR ranging between 20 and 116, increases the values of r_o approximately by a factor of 3, in comparison with the photocatalytic system without H_2O_2. This result is quite similar over the whole range investigated. The high and almost constant reaction rate for the NFR degradation within this range of H_2O_2 concentrations shows that the e^-/h^+ recombination rate was diminished by the presence of at least 25 mg L^{-1} peroxide and the photocatalytic efficiency was kept at the same level for all the oxidizing species. It is interesting to note that neither an improvement of the degradation could be associated with higher H_2O_2 concentrations, as expected, nor a decrease of the photocatalytic efficiency, as an effect of $HO^{\bullet}$ scavenging, appeared at higher concentrations.

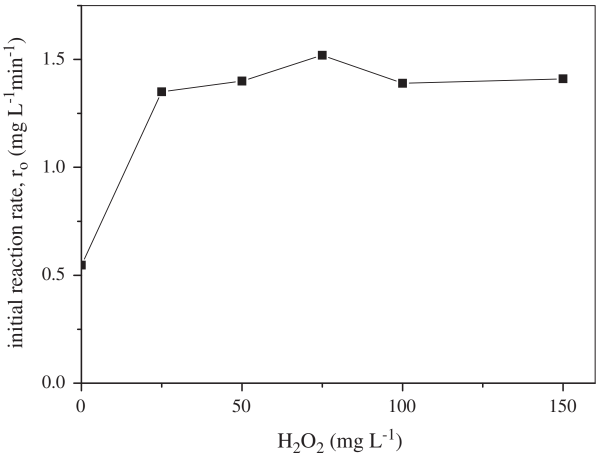

Fig. 7. Effect of concentration values of H_2O_2 on 30 mg L^{-1} NFR initial degradation rate in the presence of 0.1 g L^{-1} TiO_2 P-25 at pH 4.8.

3.4. Photodegradation products

A complete photocatalytic degradation of an organic molecule normally leads to the conversion of all its carbon atoms to gaseous CO_2, and the heteroatoms into inorganic anions, remaining mostly in the solution. In order to study the total mineralization of NFR, two sets of determinations were carried out: (a) dissolved organic carbon (DOC) reduction and (b) inorganic ions formation, as a function of irradiation time.

The overall equation, describing in principle the photocatalytic mineralization of NFR, after a long irradiation time, in the presence of excess oxygen, is presented below:

$$\begin{aligned} C_{14}H_8O_7SNNa + 15.5\,O_2 &\rightarrow [\text{intermediates}] \\ &\rightarrow 14\,CO_2 + NaNO_3 \\ &\quad + H_2SO_4 + 3\,H_2O \end{aligned} \quad (5)$$

Fig. 8 shows the degree of the dissolved organic content (DOC) reduction vs. irradiation time of an air-saturated solution containing 30 mg L^{-1} NFR in the presence of 0.1 g L^{-1} TiO_2 P-25, TiO_2 K-7000, and TiO_2-M.

In the presence of TiO_2 P-25 and Kronos 7000, around 57% of the initial carbon content in NFR was converted to CO_2 in 180 min reaction time, while the photocatalytic decomposition of the chromophore groups was almost complete, as reported in Section 3.1, Fig. 2. This suggests the generation of organic intermediate species between the first molecule splitting and the total mineralization. The full oxidation under the given experimental conditions requires a longer reaction time.

According to Eq. (5), the main final products from the photocatalytic decomposition of NFR under the given experimental conditions were CO_2, NO_3^-, NH_4^+, and SO_4^{2-}. The SO_4^{2-} amount in %, detected by ionic

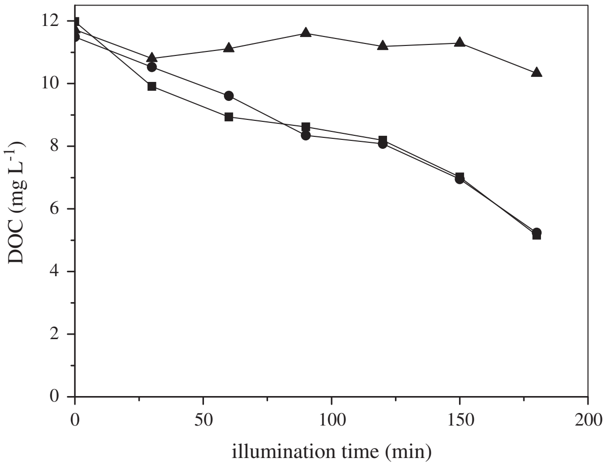

Fig. 8. Photocatalytic DOC reduction of a 30 mg L^{-1} NFR solution in the presence of 0.1 g L^{-1} (■) TiO$_2$ P-25, (●) TiO$_2$ K-7000, and (▲) TiO$_2$ M at pH 4.8.

chromatography, based on the measuring of total sulfur content in 30 mg L^{-1} NFR converted to SO_4^{2-}, as a function of the irradiation time, is given in Fig. 9. The data show that in the presence of TiO$_2$ P-25 and TiO$_2$ K-7000, 62% of the maximum theoretical amount of sulfur has been released as SO_4^{2-} from the NFR molecule after 3 h of illumination, which is in good correlation with the 57% DOC reduction. On the other hand, in the case of TiO$_2$ M with a DOC reduction of 36% after 180 min, the reaction seems to be less effective in comparison with the other two TiO$_2$ modifications, probably due to a lower BET surface area value.

In Fig. 10, the total inorganic nitrogen production is given, as a sum of nitrogen as NH_4^+, NO_2^-, and NO_3^-, during the photocatalytic degradation of 30 mg L^{-1} NFR in the presence of 0.1 g L^{-1} TiO$_2$ P 25, TiO$_2$ K-7000, and TiO$_2$ M. The nitrogen from the amino group of the initial dye molecule is transformed gradually to NH_4^+ and then to nitrite and nitrate ions. The ion chromatograph detects all three species and the sum of their N-content shows the extent of organic nitrogen conversion to the respective inorganic one. The inorganic nitrogen increases continuously and after 3 h of illumination, it reaches values corresponding to 58% in the case of TiO$_2$ P-25, 60% in the case of TiO$_2$ K-7000, and 16% in the presence of TiO$_2$-M, of the amount corresponding to complete mineralization. The main degradation product originating from nitrogen, on all three catalysts, is the ammonium ion, with after 3 h of reaction NH_4^+ to NO_3^- ratios of 6.5, 14, and 5 for TiO$_2$ P 25, TiO$_2$ K-7000, and TiO$_2$-M, respectively.

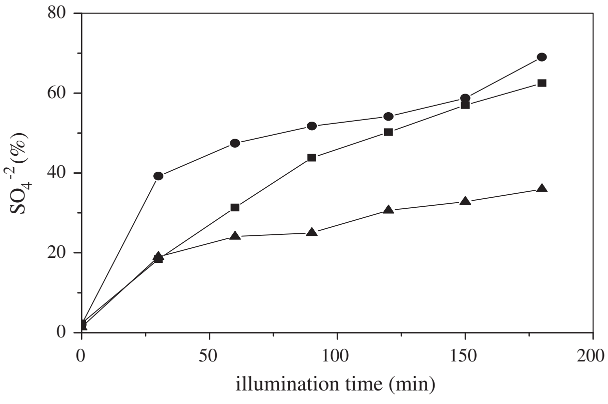

Fig. 9. Production of SO_4^{2-} by the photocatalytic degradation of 30 mg L^{-1} NFR in the presence of 0.1 g L^{-1} (■) TiO$_2$ P-25, (●) TiO$_2$ K-7000, and (▲) TiO$_2$ M at pH 4.8.

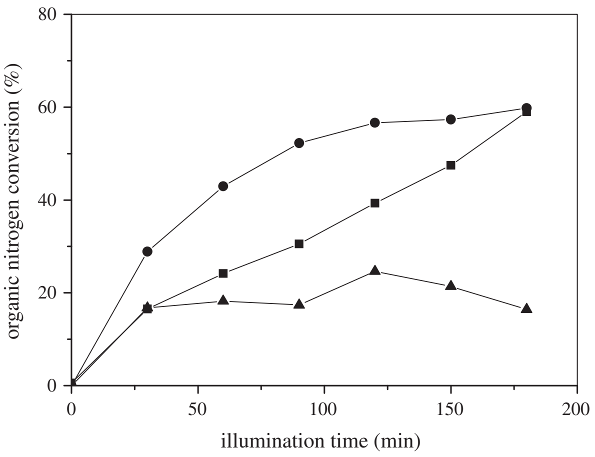

Fig. 10. Photocatalytic total inorganic nitrogen production, as a sum of nitrogen in NH_4^+, NO_2^- and NO_3^-, during the photocatalytic degradation of 30 mg L^{-1} NFR in the presence of 0.1 g L^{-1} (■) TiO$_2$ P-25, (●) TiO$_2$ K-7000, and (▲) TiO$_2$ M at pH 4.8.

The reason for NO_3^- in our case having lower concentrations, except for the catalyst nature, might as well be the low irradiation intensity, the low oxidation state of the nitrogen in NFR, as well as the short illumination time. According to G. Low et al. [31] and P. Calza et al. [32], the NH_4^+/NO_3^- ratio decreases with the increase of the irradiation time and the solution pH. The formation rate of NO_3^- is low when N is at low oxidation state, as in our case, since the conversion of NH_4^+ to NO_3^- is very slow, as predicted from the difference of 8 units in the oxidation state.

4. Conclusions

In this work, the photocatalytic degradation of NFR, an anthraquinone-derived dye, has been studied under artificial illumination. All commercial TiO$_2$ samples are efficient photocatalysts, in respect to both degradation and mineralization extent. The photo-oxidation of NFR followed first-order kinetics, which fitted the Langmuir–Hinshelwood model. Parameters such as concentration of the catalyst and initial pH play an important role affecting the reaction rate, while the addition of an electron scavenger such as hydrogen peroxide into illuminated TiO_2 suspensions leads to an enhancement of the photocatalytic process. Our study showed that the illumination of a 30 mg L^{-1} NFR solution for 3 h in the presence of 0.1 g L^{-1} TiO_2 P-25 or TiO_2 K-7000 led to total degradation and to a mineralization degree of ~57%, in agreement with the values of the sulfate and nitrogen-containing inorganic compounds monitored in the reaction system.

The photocatalytic treatment of wastewaters from the biochemical/biomedical laboratories could be employed as a powerful tool for degradation and for the reduction of organic content. The use of an inexpensive and non-toxic catalyst, such as TiO_2, and the possibility of activating it with UV-A or solar light, combined with the simple technology required for this method, can offer economically reasonable and practical solutions for the processing of this liquid waste.

Acknowledgements

This study is implemented within the framework of the Action Joint Research and Technology Programmes Greece–Romania 2011–2012 and is co-financed by the European Social Fund (ESF) and the Greek State.

References

[1] S.C. Nixon, T.J. Lack, D.T.E. Hunt, C. Lallana, A.F. Boschet, Sustainable use of Europe's water? State, prospects and issues, European Environmental Agency, Environmental Assessment Series No. 7, EEA, Copenhagen, 2000.

[2] Y. Luo, W. Guo, H.H. Ngo, L.D. Nghiem, F.I. Hai, J. Zhang, S. Liang, X.C. Wang, A review on the occurrence of micropollutants in the aquatic environment and their fate and removal during wastewater treatment, Sci. Total Environ. 473–474 (2014) 619–641.

[3] T. Deblonde, C. Cossu-Leguille, P. Hartemann, Emerging pollutants in wastewater: A review of the literature, Int. J. Hyg. Environ. Health 214 (2011) 442–448.

[4] S. Parsons, Advanced Oxidation Processes for Water and Wastewater Treatment, IWA Publishing, London, 2004.

[5] K.G. Linden, M. Mohseni, Advanced oxidation processes: Applications in drinking water treatment, reference module in earth systems and environmental sciences, Comprehensive Water Quality and Purification 2 (2014) 148–172.

[6] K. Nakata, A. Fujishima, TiO_2 photocatalysis: Design and applications, J. Photochem. Photobiol. C: Photochem. Rev. 13 (2012) 169–189.

[7] J.-M. Herrmann, Fundamentals and misconceptions in photocatalysis, J. Photochem. Photobiol. A: Chem. 216 (2010) 85–93.

[8] S. Malato, P. Fernández-Ibáñez, M.I. Maldonado, J. Blanco, W. Gernjak, Decontamination and disinfection of water by solar photocatalysis: Recent overview and trends, Catal. Today 147 (2009) 1–59.

[9] A. Bernabeu, R.F. Vercher, L. Santos-Juanes, P.J. Simón, C. Lardín, M.A. Martínez, J.A. Vicente, R. González, C. Llosá, A. Arques, A.M. Amat, Solar photocatalysis as a tertiary treatment to remove emerging pollutants from wastewater treatment plant effluents, Catal. Today 161 (2011) 235–240.

[10] F.L. Carson, Histology, A Self-Instructional Text, ASCP Press, Chicago, 1990.

[11] G. Lynn, E.B. Sansone, Destruction of Hazardous Chemicals in the Laboratory, second ed., J. Wiley and Sons Inc, New York, NY, 1994.

[12] X. Vargas, E. Tauchert, J.M. Marin, G. Restrepo, R. Dillert, D. Bahnemann, Fe-doped titanium dioxide synthesized: Photocatalytic activity and mineralization study for azo dye, J. Photochem. Photobiol. A: Chem. 243 (2012) 17–22.

[13] D. Lutic, C. Coromelci-Pastravanu, I. Cretescu, I. Poulios, C.D. Stan, Photocatalytic treatment of rhodamine 6G in wastewater using photoactive ZnO, Int. J. Photoenergy 2012 (2012) 8pp. (Article ID 475131).

[14] A. Khanna, K.V. Shetty, Solar photocatalysis for treatment of Acid Yellow-17 (AY-17) dye contaminated water using Ag@TiO_2 core-shell structured nanoparticles, Environ. Sci. Pollut. Res. 20 (2013) 5692–5707.

[15] J.G. McEnvoy, W. Cui, Z. Zhang, Synthesis and characterization of Ag/AgCl-activated carbon composites for enhanced visible light photocatalysis, Appl. Catal. B Environ. 144 (2014) 702–712.

[16] N. Riaz, F.K. Chong, Z.B. Man, M. Saqib Khan, B.K. Dutta, Photodegradation of orange II under visible light using Cu–Ni/TiO_2: Influence of Cu:Ni mass composition, preparation, and calcination temperature, Ind. Eng. Chem. Res. 52 (2013) 4491–4503.

[17] M. Sioi, A. Bolosis, E. Kostopoulou, I. Poulios, Photocatalytic treatment of colored wastewater from medical laboratories: Photocatalytic oxidation of hematoxylin, J. Photochem. Photobiol. A: Chem. 184 (2006) 18–25.

[18] I. Poulios, E. Micropoulou, R. Panou, E. Kostopoulou, Photooxidation of eosin Y in the presence of semiconducting oxides, Appl. Catal. B: Environ. 41 (2003) 345–355.

[19] A.M. Braun, M. Maurette, E. Oliveros, Photochemical Technology, Wiley, New York, NY, 1991.

[20] S. Parra, J. Olivero, C. Pulgarin, Relationships between physicochemical properties and photoreactivity of four biorecalcitrant phenylurea herbicides in aqueous TiO_2 suspension, Appl. Catal. B: Environ. 36 (2002) 75.

[21] S. Kaniou, K. Pitarakis, I. Barlagianni, I. Poulios, Photocatalytic oxidation of sulfamethazine, Chemosphere 60 (2005) 372–380.

[22] D. Robert, B. Dongui, J.-V. Weber, Heterogeneous photocatalytic degradation of 3-nitroacetophenone in TiO_2 aqueous suspension, J. Photochem. Photobiol. A: Chem. 156 (2003) 195–200.

[23] J. Cunningham, G. Al-Sayyed, S. Srijaranai, Adsorption of model pollutants onto TiO_2 particles in relation to photoremedation of contaminated water, in: G. Helz, R. Zepp, D. Crosby (Eds.), Aquatic and Surface Photochemistry, Lewis Publs., CRC Press, 1994, Chap. 22, pp. 317–348.

[24] B. Zielińska, J. Grzechulska, R.J. Kaleńczuk, A.W. Morawski, The pH influence on photocatalytic decomposition of organic dyes over A11 and P25 titanium dioxide, Appl. Catal. B: Environ. 45 (2003) 293–300.

[25] W. Chu, W.K. Choy, T.Y. So, The effect of solution pH and peroxide in the TiO_2-induced photocatalysis of chlorinated aniline, J. Hazard. Mater. 141 (2007) 86–91.

[26] N. Philippidis, S. Sotiropoulos, A. Efstathiou, I. Poulios, Photoelectrocatalytic degradation of the insecticide imidacloprid using TiO_2/Ti electrodes, J. Photochem. Photobiol. A: Chem. 204 (2009) 129–136.

[27] S. Helali, F. Dappozze, S. Horikoshi, T.H. Bui, N. Perol, C. Guillard, Kinetics of the photocatalytic degradation of methylamine: Influence of pH and UV-A/UV-B radiant fluxes, J. Photochem. Photobiol. A: Chem. 255 (2013) 50–57.

[28] S. Malato, J. Blanco, M.I. Maldonado, P. Fernández-Ibáñez, A. Campos, Optimising solar photocatalytic mineralisation of pesticides by adding inorganic oxidising species; application to the recycling of pesticide containers, Appl. Catal. B: Environ. 28 (2000) 163–174.

[29] V. Kitsiou, N. Filippidis, D. Mantzavinos, I. Poulios, Heterogeneous and homogeneous photocatalytic degradation of the insecticide imidacloprid in aqueous solutions, Appl. Catal. B: Environ. 86 (2009) 27–35.

[30] D.D. Dionysiou, M.T. Suidan, I. Baudin, J.M. Laîné, Effect of hydrogen peroxide on the destruction of organic contaminants-synergism and inhibition in a continuous mode photocatalytic reactor, Appl. Catal. B: Environ. 50 (2004) 259–269.

[31] G.K.C. Low, S.R. McEvoy, R.W. Matthews, Formation of nitrate and ammonium ions in titanium dioxide mediated photocatalytic degradation of organic compounds containing nitrogen atoms, Environ. Sci. Technol. 25 (1991) 460–467.

[32] P. Calza, E. Pelizzetti, C. Minero, The fate of organic nitrogen in photocatalysis: An overview, J. Appl. Electrochem. 35 (2005) 665–673.